Contribution from the Department of Chemistry,
University of Houston, Houston, Texas 77004

Nature of the Axial Bond between Dimethyl Sulfoxide and a Series of Dirhodium Complexes

M. Y. Chavan, X. Q. Lin, M. Q. Ahsan, I. Bernal,* J. L. Bear,* and K. M. Kadish*

Received September 25, 1985

Dirhodium complexes of the form $Rh_2(ac)_n(acam)_{4-n}(L)(L')$, where L, L' = acetonitrile (AN), dimethyl sulfoxide (Me_2SO), ac = CH_3COO^-, acam = CH_3CONH^-, were structurally, spectrally, and electrochemically characterized. The derivative with L = L' = Me_2SO crystallizes in the space group $P\bar{1}$ with cell constants of a = 8.743 (2) Å, b = 8.970 (3) Å, c = 8.353 (2) Å, α = 104.04 (2)°, β = 93.43 (4)°, γ = 115.52 (3)°, V = 563.34 Å^3, and d = 1.858 (calculated for Z = 1). The structural analysis converged to R = 0.0245 and R_w = 0.0362. In neat acetonitrile, the dirhodium complexes existed as bis(acetonitrile) adducts, but when dimethyl sulfoxide was added to solution, $Rh_2(ac)_n(acam)_{4-n}(Me_2SO)(AN)$ and $Rh_2(ac)_n(acam)_{4-n}(Me_2SO)_2$ were formed stepwise. Stability constants for these ligand-exchange reactions were calculated, and a crystal structure of $Rh_2(acam)_4(Me_2SO)_2$ was determined. The various ligated $Rh_2(ac)_n(acam)_{4-n}$ complexes were oxidized to give ligated $[Rh_2(ac)_n(acam)_{4-n}]^+$ species, and these reactions were electrochemically investigated in solutions containing different Me_2SO/acetonitrile ratios. Formation constants for the ligand-exchange reactions of the oxidized and reduced complexes were determined with use of spectral and electrochemical methodologies. Electrooxidation mechanisms were also determined for each of the $Rh_2(ac)_n(acam)_{4-n}$ species as a function of the Me_2SO/AN ratio, and trends of binding constants were examined as functions of the number of acetamidate bridging ligands in the complex. An analysis of these data led to the conclusion that different modes of Me_2SO binding (via sulfur or oxygen) exist as a function of the specific oxidation state of the dirhodium complex (zero or +1) and the particular combination of acetate and acetamidate bridging ligands. Finally, all of these results were discussed in terms of hardness and softness of the acid–base pairs as well as in terms of possible π interaction between the dirhodium centers and the sulfur-bound Me_2SO molecule.

Introduction

Dinuclear rhodium(II) carboxylates form axial adducts with a wide variety of ligand types ranging from pure σ donors to traditionally π-acid ligands.[1] In the case of π-acid ligands, it is not clear if the axial interaction is primarily σ in nature or whether significant Rh → axial ligand π back-donation also occurs. In principle, both σ- and π-type interactions are possible. Structural[2,3] and theoretical[4] studies have been carried out on a variety of complexes involving π-acid ligands, and in general, the conclusion has been that there is at most only a minor π contribution involved in the axial bond. In contrast, Drago and co-workers[5] have proposed the existance of π back-bonding in several adducts of dirhodium tetrabutyrate. The proposal is based on thermodynamic data for adduct formation reactions of dirhodium complexes as well as on electrochemical studies.

One of the difficulties in determining the presence or absence of π bonding in dirhodium carboxylates is the limited basicity range of carboxylate bridging ligands. The electron density on the dirhodium center can be decreased by substituting electron-withdrawing groups such as CF_3 for alkyl groups on the carboxylate;[6] however, the electron density cannot be increased much above that present in the tetraacetate complex.

Recently, a series of $Rh_2(ac)_n(acam)_{4-n}$ complexes (where ac = CH_3COO^-, acam = CH_3CONH^-, and n varies from 0 to 4) have been studied electrochemically and spectroscopically, as well as by ESR techniques.[7] In this series of complexes, the electron density of the dirhodium(II) center increases as n decreases. Therefore, the π-donor ability of the rhodium dimer may also increase with decreasing n value.

Interesting results have emerged from the electrochemical study of $Rh_2(ac)_n(acam)_{4-n}$ in different solvent systems.[7] Gutmann donor numbers (DN)[8] correlate with half-wave potentials for the oxidation of the dirhodium(II) carboxylates in acetonitrile (AN), pyridine (py), and dimethyl sulfoxide (Me_2SO). However, a relatively large positive deviation from the DN-based trend of half-wave potentials is observed in Me_2SO for $Rh_2(ac)_n(acam)_{4-n}$ where n = 0, 1.[7] These results suggest a difference in the Rh–axial ligand interaction for the carboxylate and acetamidate complexes in Me_2SO.

The ambidentate nature of Me_2SO in axial binding to metal–metal-bonded dirhodium carboxylates has been demonstrated crystallographically by Cotton and Felthouse.[9,10] Prior to this study, color correlations were used to suggest the mode of binding. It was proposed that in Me_2SO yellow solutions of dirhodium carboxylates suggested Me_2SO axial ligation via the sulfur atom while blue solutions of dirhodium carboxylates in Me_2SO implied Me_2SO binding via the oxygen atom.[11]

The preference for axial binding via sulfur or oxygen atoms in dirhodium carboxylates is clearly dependent upon the nature of the substituent, R, on the carboxylate bridging ligands, RCO_2^-. When R is highly electron withdrawing (e.g. R = CF_3), the dirhodium(II,II) complex prefers Me_2SO binding via the oxygen atom, while for R = CH_3, C_2H_5, etc., Me_2SO axial binding is preferred via the sulfur atom. Hence, such preferences for the mode of axial binding of Me_2SO have been linked[10] to the "softness" or "hardness" of the dirhodium complex itself. There may also be changes in magnitude of the S vs. O bonding mode preference on going from solid crystals to liquid solutions as well as with changes in the oxidation state(s) of rhodium centers (i.e., Rh^{IV}_2, Rh^{V}_2, or Rh^{VI}_2). This latter possibility is suggested by results of electrochemical and ESR studies of the oxidized dirhodium complexes $[Rh_2(ac)_n(acam)_{4-n}]^+$.[7]

In this present study we have determined the crystal and molecular structure of $Rh_2(acam)_4(Me_2SO)_2 \cdot 2H_2O$ in order to evaluate the nature of the Rh–axial ligand bonds relative to that in $Rh_2(ac)_4(Me_2SO)_2$. In addition, we have examined the possibility that mixed binding modes exist for Me_2SO adducts of various dirhodium complexes by measuring the formation constants of such adducts. Formation constants for Me_2SO addition were measured for both the neutral and the oxidized forms of the complexes. These determinations were carried out by both optical (spectrophotometric) and electrochemical methods.

Experimental Section

Chemicals. $Rh_2(ac)_n(acam)_{4-n}$ complexes (where n = 0–4) were synthesized by the stepwise exchange reaction of $Rh_2(ac)_4$ with acetamidate ligands.[7] Five compounds were investigated in this study. These were $Rh_2(ac)_4$, $Rh_2(ac)_3(acam)$, $Rh_2(ac)_2(acam)_2$, $Rh_2(ac)(acam)_3$, and $Rh_2(acam)_4$. Different isomers have been suggested to exist only for the compound $Rh_2(ac)_2(acam)_2$. In the present study these isomers have not

(1) Felthouse, T. R. *Prog. Inorg. Chem.* **1982**, *29*, 73 and references therein.
(2) Christoph, G. G.; Halpern, J.; Khare, G. P.; Koh, Y. B.; Ramanowski, C. *Inorg. Chem.* **1981**, *20*, 3029.
(3) Christoph, G. G.; Koh, Y. B. *J. Am. Chem. Soc.* **1979**, *101*, 1422.
(4) Bursten, B. E.; Cotton, F. A. *Inorg. Chem.* **1981**, *20*, 3042.
(5) Drago, R. S.; Tanner, S. P.; Richman, R. M.; Long, J. R. *J. Am. Chem. Soc.* **1979**, *101*, 2897.
(6) Das, K.; Kadish, K. M.; Bear, J. L. *Inorg. Chem.* **1978**, *17*, 930.
(7) Chavan, M. Y.; Zhu, T. P.; Lin, X. Q.; Ahsan, M. Q.; Bear, J. L.; Kadish, K. M. *Inorg. Chem.* **1984**, *23*, 4538.
(8) Gutmann, V. *The Donor Acceptor Approach to Molecular Interactions* Plenum: New York, 1978.
(9) Cotton, F. A.; Felthouse, T. *Inorg. Chem.* **1980**, *19*, 323.
(10) Cotton, F. A.; Felthouse, T. *Inorg. Chem.* **1980**, *19*, 2347.
(11) Kitchens, J.; Bear, J. L. *Thermochim. Acta* **1970**, *1*, 537.

0020-1669/86/1325-1281$01.50/0

Table I. Summary of Data Collection and Processing Parameters

space group	$P\bar{1}$
cell constants	a = 8.743 (2) Å
	b = 8.970 (3) Å
	c = 8.353 (2) Å
	α = 104.04 (2)°
	β = 93.43 (4)°
	γ = 115.52 (3)°
cell vol	V = 563.34 Å^3
molecular formula	$C_{12}H_{32}N_4O_8S_2Rh_2$
mol wt	630.341
density (calcd, Z = 1)	1.858 g cm^{-3}
radiation	Mo Kα (λ = 0.71073 Å)
abs coeff	μ = 16.6 cm^{-1}
rel transmission coeff	1.000–0.783
data collection range	$4.0 \le 2\theta \le 74.0$
scan width	$\Delta\theta = (1.0 + 0.35 \tan\theta)°$
max scan time	180 s
scan speed range	0.50–6.70 deg min^{-1}
total data collected	5226
data with $I = 3\sigma(I)$[a]	4883
total variables	186
$R = \sum\|\|F_o\| - \|F_c\|\|/\sum\|F_o\|$	0.0245
$R_w = [\sum w(\|F_o\| - \|F_c\|)^2/\sum w\|F_o\|^2]^{1/2}$	0.0362
weights	$w = [\sigma(F_o)]^{-2}$

[a] The difference between total data collected and this number is due to subtraction of standards, redundant data, and those data that do not meet the criterion of having $I \ge 3\sigma(I)$.

been resolved, but analysis of the electrochemical data indicated little or no difference in their redox properties.

Acetonitrile (AN) and dimethyl sulfoxide (Me_2SO) were purchased as reagent grade from Burdick and Jackson, stored over 4-Å molecular sieves, and used without further purification. Other chemicals were analytical grade and were used without further purification. Tetra-*n*-butylammonium perchlorate, TBAP (Fluka), was recrystallized from ethanol–hexane and dried in a vacuum oven prior to use.

Crystallographic Data Collection and Processing. A purple-red, diamond-shaped plate was selected for data collection, mounted on a glass pin, and sprayed with Krylon in order to prevent loss of water of hydration, known to occur in related substances. It was then mounted on an Enraf-Nonius CAD-4 diffractometer located in a room kept at 14.5 °C and ca. 60% humidity. All calculations were carried out with the SDP-PLUS (Dec 1982 update) series of programs.[12]

The crystal was aligned with use of 25 reflections. From the cell constants and the Niggli matrix, it was determined that the substance crystallizes in the triclinic system. Since the value of Z = 1, it was possible for the space group to be $P1$. However, the distribution of intensities derived from NORMAL and NZTEST programs strongly suggest the centrosymmetric choice, $P\bar{1}$, to be the correct one.

A total of 5226 data of the forms $\pm h,\pm k,l$ were collected in the range $4° \le 2\theta \le 74°$ with use of the data collection parameters listed in Table I. The data were corrected for absorption by using an empirical correction curve derived from ψ scans of reflections (1,10,−1), (5,−1,0), (−8,1,0), (−10,1,0), (−12,1,0), and (12,−2,1) located between 80 and 90° in 2θ. ψ-scan data were collected in 37 steps of 10°. Relative transmission coefficients ranged from 1.000 to 0.783.

The Rh atom was obtained from a Patterson function, and all nonhydrogen atoms appeared in the first difference map. A difference map, computed after the heavy atoms were anisotropically refined, revealed the positions of all of the hydrogen atoms. Further refinement showed that, while the positional parameters of all hydrogens could be refined to chemically reasonable positions, not all of the isotropic thermal parameters had sensible values. Therefore, those with large, unreasonable values had their thermal parameters fixed at 4.0 Å.[12] Table II, listing the final positions and thermal parameters of the atoms, shows which these were since no error is quoted for them. The SPD system uses the hydrogen scattering curve of Stewart et al.[13] and, for the other atoms, those of Cromer and Mann.[14] Refinement converged to unweighted and weighted R values of 0.025 and 0.0362, respectively, with use of the entire set of 4883 observed data.

(12) TEXRAY 230 programs for the Enraf-Nonius CAD-4 diffractometer were obtained from the Molecular Structure Corp., College Station, TX 77840.
(13) Stewart, R. F.; Davidson, E. R.; Simpson, W. T. *J. Chem. Phys.* **1965**, *42*, 3175.
(14) Cromer, D. T.; Mann, J. B. *Acta Crystallogr., Sect. A: Cryst. Phys., Diffr., Theor. Gen. Crystallogr.* **1968**, *A24*, 321.

Table II. Positional Parameters and Their Estimated Standard Deviations

atom	x	y	z	B,[a] Å^3
Rh	0.44150 (1)	0.34316 (1)	0.43812 (1)	1.565 (2)
S1	0.33395 (4)	0.03830 (4)	0.29849 (5)	2.085 (6)
OW1	0.0906 (2)	−0.0495 (2)	0.6667 (2)	4.73 (4)
O1	0.2193 (1)	0.3341 (1)	0.3251 (1)	2.29 (2)
O2	0.5518 (1)	0.3855 (1)	0.2301 (1)	2.38 (2)
O3	0.2411 (2)	−0.0990 (1)	0.3795 (2)	3.62 (3)
N1	0.3349 (1)	0.6256 (1)	0.4429 (2)	2.18 (2)
N2	0.6629 (2)	0.6753 (1)	0.3547 (2)	2.37 (2)
C1	0.2098 (2)	0.4775 (2)	0.3524 (2)	1.98 (2)
C2	0.0438 (2)	0.4663 (2)	0.2748 (2)	2.84 (3)
C3	0.3570 (2)	0.4577 (2)	0.7680 (2)	2.07 (2)
C4	0.7288 (2)	0.5705 (2)	0.0836 (2)	3.06 (3)
C5	0.5057 (2)	0.0003 (2)	0.2286 (3)	3.51 (4)
C6	0.2035 (2)	−0.0166 (3)	0.1017 (3)	3.73 (4)
HN1	0.324 (2)	0.717 (2)	0.431 (2)	2.2 (4)
HN2	0.733 (2)	0.778 (2)	0.344 (2)	2.6 (4)
H2A	0.051 (2)	0.588 (2)	0.318 (3)	3.9 (5)
H2B	−0.002 (2)	0.390 (2)	0.170 (3)	4*
H2C	−0.056 (2)	0.367 (2)	0.307 (3)	4.7 (6)*
H4A	0.853 (3)	0.692 (3)	0.118 (4)	7.7 (8)*
H4B	0.766 (2)	0.493 (2)	0.039 (3)	4*
H4C	0.680 (3)	0.591 (3)	0.014 (3)	5.6 (6)*
H5A	0.441 (2)	−0.116 (2)	0.138 (3)	4.2 (5)*
H5B	0.550 (2)	0.071 (2)	0.180 (3)	3.7 (5)*
H5C	0.586 (3)	0.014 (3)	0.323 (3)	6.7 (7)*
H6A	0.235 (3)	0.041 (3)	0.045 (3)	5.4 (6)*
H6B	0.185 (2)	−0.119 (2)	0.039 (2)	3.3 (4)*
H6C	0.110 (3)	0.004 (3)	0.109 (3)	6.9 (7)*
HW1	0.109	−0.084	0.541	4*
HW2	0.000	−0.139	0.668	4*

[a] Starred atoms were refined isotropically. Anisotropically refined atoms are given in the form of the isotropic equivalent thermal parameter defined as $^4/_3[a^2B_{11} + b^2B_{22} + c^2B_{33} + ab(\cos\gamma)B_{12} + ac(\cos\beta)B_{13} + bc(\cos\alpha)B_{23}]$.

Tables listing the anisotropic thermal parameters and the structure factors are included as supplementary material. The bond distances, bond angles, and torsional angles are listed in Tables III–V, respectively.

Instrumentation. Cyclic voltammetric measurements were made on a Princeton Applied Research (PAR) 174 or 173/175 polarograph/potentiostat system or an IBM EC 225 voltammetric analyzer utilizing a three-electrode system. The working electrode consisted of a platinum button. An IBM commercial saturated calomel electrode (SCE) was used as the reference electrode, and a platinum wire was used as the auxiliary electrode. The reference electrode was separated from the bulk of the solution by a bridge containing the same solvent and supporting electrolyte. Solutions in the bridge were changed periodically. Potentials were measured vs. SCE. The total solution volume utilized for electrochemical experiments was 5–10 mL, and the concentration of $Rh_2(ac)_n(acam)_{4-n}$ was $\sim 10^{-3}$ M.

An IBM Model 9430 spectrophotometer was used to obtain electronic absorption spectra of the complexes.

Results and Discussion

The crystal structure of $Rh_2(acam)_4(Me_2SO)_2$ was investigated in order to compare the Rh–S and Rh–Rh distances with those in $Rh_2(ac)_4(Me_2SO)_2$. Figure 1 shows a model of the $Rh_2(acam)_4(Me_2SO)_2$ molecule. The labels correspond to the numbering system used in the crystallographic analysis. Four acetamidato ligands surround a metal–metal-bonded Rh–Rh moiety, and each Rh is axially ligated by a dimethyl sulfoxide molecule. The equatorial ligand arrangement is identical with that found in the case of the closely related $Rh_2(acam)_4(H_2O)_2$ complex described elsewhere.[16]

The hydrogens on the acetamidate nitrogens are shown in their refined positions, and they serve to distinguish the N vs. the O attachment of the ligand to the Rh atoms. We have demonstrated in three previous cases[15-17] that there is a well-defined difference between the Rh–O and the Rh–N bonds of about 0.06–0.07 Å,

(15) Dennis, A. M.; Korp, J. D.; Bernal, I.; Howard, R. A.; Bear, J. L. *Inorg. Chem.* **1983**, *22*, 1522.
(16) Ahsan, M. Q.; Bernal, I.; Bear, J. L. *Inorg. Chem.* **1986**, *25*, 260.
(17) Ahsan, M. Q.; Bernal, I.; Bear, J. L. *Inorg. Chim. Acta*, in press.

Table III. Bond Distances (Å)[a]

atom 1	atom 2	dist	atom 1	atom 2	dist	atom 1	atom 2	dist
Rh	Rh	2.452 (0)	C1	C2	1.506 (1)	C4	H4B	0.904 (12)
Rh	S1	2.414 (0)	OW1	HW1	1.064 (1)	C4	H4C	0.805 (14)
Rh	O1	2.069 (1)	OW1	HW2	0.852 (1)	C5	H5A	1.019 (12)
Rh	O2	2.073 (1)	O1	C1	1.290 (1)	C5	H5B	0.802 (11)
Rh	N1	2.012 (1)	N1	C1	1.301 (1)	C5	H5C	0.975 (15)
Rh	N2	2.013 (1)	N1	HN1	0.891 (9)	C6	H6A	0.761 (13)
S1	O3	1.498 (1)	N2	HN2	0.891 (10)	C6	H6B	0.880 (11)
S1	C5	1.778 (1)	C2	H2A	1.036 (11)	C6	H6C	0.911 (14)
S1	C6	1.773 (1)	C2	H2B	0.910 (12)	O1	HW2	1.980 (1)
O1	C1	1.290 (1)	C2	H2C	1.050 (12)	O3	HW1	1.842 (1)
N1	C1	1.301 (1)	C4	H4A	1.11 (2)			

[a] Numbers in parentheses are estimated standard deviations in the least significant digits.

Table IV. Bond Angles (deg)[a]

atom 1	atom 2	atom 3	angle	atom 1	atom 2	atom 3	angle	atom 1	atom 2	atom 3	angle
Rh	Rh	S1	175.92 (0)	O2	Rh	N1	90.00 (9)	H2A	C2	H2B	128 (1)
Rh	Rh	O1	89.53 (1)	O2	Rh	N2	174.65 (2)	H2A	C2	H2C	115.5 (8)
Rh	Rh	O2	89.32 (2)	N1	Rh	N2	91.24 (3)	H2B	C2	H2C	82.3
Rh	Rh	N1	85.43 (2)	O3	S1	C5	105.80 (5)	H4A	C4	H4B	100
Rh	Rh	N2	85.59 (2)	O3	S1	C6	107.57 (5)	H4A	C4	H4C	99 (1)
S1	Rh	O1	90.10 (2)	C5	S1	C6	99.69 (6)	H4B	C4	H4C	113
S1	Rh	O2	86.62 (2)	O1	C1	N1	122.86 (6)	H5A	C5	H5B	106 (1)
S1	Rh	N1	94.93 (2)	O1	C1	C2	116.51 (6)	H5A	C5	H5C	120 (1)
S1	Rh	N2	98.45 (2)	N1	C1	C2	120.64 (6)	H5B	C5	H5C	112 (1)
O1	Rh	O2	90.08 (2)	HW1	OW1	HW2	102.47	H6A	C6	H6B	104 (1)
O1	Rh	N1	174.96 (2)	C1	N1	HN1	114.1 (6)	H6A	C6	H6C	90 (1)
O1	Rh	N2	88.23 (3)	O1	C1	N1	122.86 (6)	H6B	C6	H6C	117 (1)

[a] Numbers in parentheses are estimated standard deviations in the least significant digits.

Table V. Torsional Angles (deg)

atom 1	atom 2	atom 3	atom 4	angle	atom 1	atom 2	atom 3	atom 4	angle
O1	Rh	S1	O3	−95.6	Rh	S1	C6	H6B	165.8
O1	Rh	S1	C5	139.5	Rh	S1	C6	H6C	−60.1
O1	Rh	S1	C6	31.5	O3	S1	C6	H6A	−179.2
O2	Rh	S1	O3	174.3	O3	S1	C6	H6B	−58.8
O2	Rh	S1	C5	49.5	O3	S1	C6	H6C	75.4
O2	Rh	S1	C6	−58.5	C5	S1	C6	H6A	−69.1
S1	Rh	O1	C1	−176.8	C5	S1	C6	H6B	51.3
O2	Rh	O1	C1	−90.2	C5	S1	C6	H6C	−174.5
Rh	S1	C5	H5A	−160.0	Rh	O1	C1	N1	2.0
Rh	S1	C5	H5B	−49.3	Rh	O1	C1	C2	−177.5
Rh	S1	C5	H5C	71.2	HN1	N1	C1	O1	165.2
O3	S1	C5	H5A	65.6	HN1	N1	C1	C2	−15.4
O3	S1	C5	H5B	176.4	O1	C1	C2	H2A	174.3
O3	S1	C5	H5C	−63.2	O1	C1	C2	H2B	−38.8
C6	S1	C5	H5A	−45.9	O1	C1	C2	H2C	50.0
C6	S1	C5	H5B	64.9	N1	C1	C2	H2A	−5.2
C6	S1	C5	H5C	−174.7	N1	C1	C2	H2B	141.7
Rh	S1	C6	H6A	45.3	N1	C1	C2	H2C	−129.5

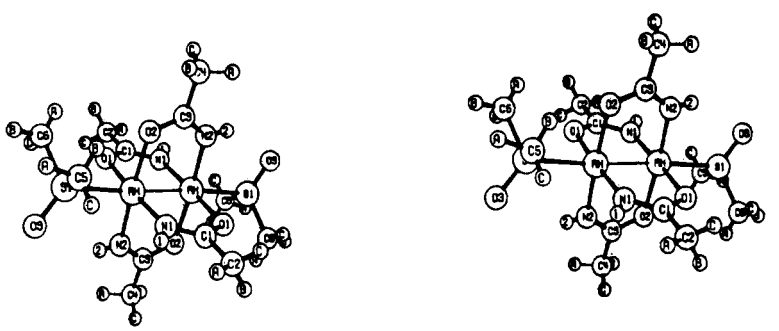

Figure 1. Stereoview of the $Rh_2(acam)_4(Me_2SO)_2$ molecule displaying the numbering system used for crystallographic analysis.

the latter being the shorter. This observation is confirmed in the present study and identifies this species as having two nitrogens cis to one another at each Rh atom. We have shown previously[16,17] the significance of this result to the mechanism of acetamidato-for-acetate substitution in preparation of these compounds.

Bonding within the Molecule. The two independent Rh–N distances are 2.012 (1) and 2.013 (1) Å, while the two Rh–O distances are 2.069 (1) and 2.073 (1) Å. There is a considerable internal consistency within this structural determination and with the results reported for related species,[15–17] where typical (average) values for Rh–N and Rh–O bonds were 2.008 (2) and 2.073 (2) Å, respectively.[16,17]

The most important contribution of the present structural determination to the general theme of this paper is the value of

the Rh–S distance. As shown in Table VI, the Rh–OH_2 bond length for $Rh_2(acam)_4(H_2O)_2$ is 0.043 Å, longer than that reported for $Rh_2(ac)_4(H_2O)_2$.[16,18] The Rh–Rh bond distance is also longer for the acetamidate complex (0.029 Å) even though the axial water interaction is weaker. It is obvious that both the bridging and axial ligand affect the Rh–Rh bond distance. A different trend is observed in the Rh–S bond lengths of the two dirhodium(II) complexes containing bound Me_2SO. In $Rh_2(ac)_4(Me_2SO)_2$ the Rh–S bond distance is 2.451 Å while in $Rh_2(acam)_4(Me_2SO)_2$ it is 2.414 Å. Again, however, the Rh–Rh bond distance for the acetamide complex is longer. The short Rh–S bond found for the electron-rich acetamidate complex could be due to an increase in the Rh→S π component of the Rh–S axial bond or could simply result from a stronger Rh←S σ interaction due to $Rh_2(acam)_4$ being a considerably softer acid. If both Rh←S σ and Rh→S π interactions are significant in the Rh–S axial bond, the σ interaction should increase the Rh–Rh bond distance whereas the opposite would be true for the π interaction. Theoretical calculations[19] on the dirhodium carboxylates predict a single σ bond between the two rhodium ions. Therefore, the Rh–Rh bond distance should be more sensitive to the Rh←S σ contribution to the bond. Since an increase in the Rh→S π interaction should also increase the magnitude of the Rh←S σ component through synergism, it is not possible to use the Rh–Rh bond distance to draw inferences about the presence or the absence of π interaction in the Rh–S bond.

Spectroscopic Monitoring of Me_2SO Binding to Neutral and Singly Oxidized $Rh_2(ac)_n(acam)_{4-n}$ Complexes. The crystal structure (discussed above) shows the increased strength of the Rh–S bond on going from $Rh_2(ac)_4(Me_2SO)_2$ to $Rh_2(acam)_4(Me_2SO)_2$. However, a comparison of Me_2SO binding constants for the neutral and singly oxidized complexes should help to understand if the Rh–S interactions involve primarily σ-donor Me_2SO ligands. These binding constants were measured in this study.

Dirhodium(II) complexes with acetamidate bridging ligands are insoluble in weakly binding solvents such as dichloromethane and acetone. Hence, acetonitrile (AN) was chosen as the medium for studying Me_2SO binding properties of the dirhodium complexes. The spectra of $[Rh_2(ac)_n(acam)_{4-n}]^{0/+}$ in AN and Me_2SO have been reported.[7] In both solvents, the complexes are bound with two solvent molecules. Thus, equilibrium constants (K_1, K_2, and β_2) for Me_2SO binding to Rh(II) and $Rh(II^1/_2)$ involve a displacement of AN as shown in eq 1–3 for the neutral complexes and eq 4–6 for the singly oxidized species. In both sets of equations L represents the $(ac)_n(acam)_{4-n}$ ligands taken together.

$$Rh_2L(AN)_2 + Me_2SO \overset{K_1}{\rightleftharpoons} Rh_2L(AN)(Me_2SO) + AN \quad (1)$$

$$Rh_2L(AN)(Me_2SO) + Me_2SO \overset{K_2}{\rightleftharpoons} Rh_2L(Me_2SO)_2 + AN \quad (2)$$

$$Rh_2L(AN)_2 + 2Me_2SO \overset{\beta_2}{\rightleftharpoons} Rh_2L(Me_2SO)_2 + 2AN \quad (3)$$

$$[Rh_2L(AN)_2]^+ + Me_2SO \overset{K_1^+}{\rightleftharpoons} [Rh_2L(AN)(Me_2SO)]^+ + AN \quad (4)$$

$$[Rh_2L(AN)(Me_2SO)]^+ + Me_2SO \overset{K_2^+}{\rightleftharpoons} [Rh_2L(Me_2SO)_2]^+ + AN \quad (5)$$

$$[Rh_2L(AN)_2]^+ + 2Me_2SO \overset{\beta_2^+}{\rightleftharpoons} [Rh_2L(Me_2SO)_2]^+ + 2AN \quad (6)$$

In order to avoid dilution effects, AN solutions of $Rh_2(ac)_n(acam)_{4-n}$ were titrated with Me_2SO containing the same concentration of the dirhodium complex and Me_2SO solutions of $Rh_2(ac)_n(acam)_{4-n}$ were titrated with AN containing the same concentration of dirhodium complex.

Table VI. Comparison of Rh–Rh and Rh–L Bond Distances as a Function of Axial and Bridging Ligands

	bond length, Å			
	Rh–Rh		Rh–O	Rh–S
compd	H_2O	Me_2SO	H_2O	Me_2SO
$Rh_2(acam)_4$	2.415[c]	2.452	2.353[c]	2.414
$Rh_2(ac)_4$	2.386[a]	2.406[b]	2.310[a]	2.451[b]

[a] Reference 18. [b] Reference 9. [c] Reference 16.

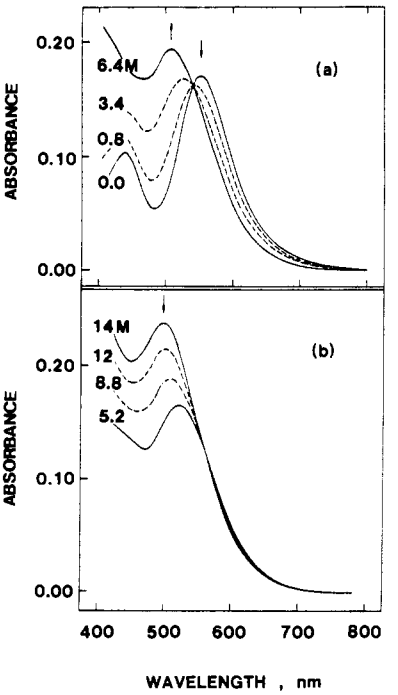

Figure 2. Spectral changes of $Rh_2(ac)_4$ (a) in acetonitrile (0.1 M TBAP) upon Me_2SO additions and (b) in Me_2SO (0.1 M TBAP) upon acetonitrile additions. Concentrations of Me_2SO are denoted on each spectrum.

The spectral changes observed during an Me_2SO titration of $Rh_2(ac)_4$ in AN are shown in Figure 2. At low concentrations of Me_2SO there is a single isosbestic point, which occurs at about 540 nm (Figure 2a). However, when the concentration of Me_2SO becomes higher than 3.4 M, a new isosbestic point appears at about 560 nm. Over the remaining range of increasing [Me_2SO], the band originally at 550 nm in pure acetonitrile shifts continuously until a peak maximum is reached at 500 nm. No new absorbance peaks appear in the visible region.

To determine the presence of a second Me_2SO binding step (giving a bis(dimethyl sulfoxide) adduct), a back-titration was conducted with AN as the titrant. The spectral changes for this reaction are shown in Figure 2b. A well-defined isosbestic point appeared at 560 nm while the original peak at ~500 nm shifted to lower energy and lost intensity with increasing [AN]. This confirms the second Me_2SO binding step at higher Me_2SO concentrations, but the binding constant is seen to be small. Analysis of the competition between Me_2SO binding and AN binding gave Me_2SO binding constants of log K_1 = 1.04 and log K_2 = −0.22. The specific reactions for which these log K values apply are given by eq 1 and 2.

Figure 3 shows the results for titration of $Rh_2(acam)_4$ in AN with Me_2SO. Two sets of isosbestic points are observed at different concentrations of titrant. This indicates the stepwise formation of mono- and bis(dimethyl sulfoxide) adducts. No specific absorption peak wavelength can be attributed to the monoadduct because the final spectrum for $Rh_2L(AN)(Me_2SO)$ (Figure 3a or the initial spectrum in Figure 3b) can only be estimated by the disappearance of the first isosbestic point and the appearance of the second isosbestic point.

(18) Cotton, F. A.; DeBaer, B. G.; La Prade, M. D.; Pipal, J. R.; Ucko, D. A. *J. Am. Chem. Soc.* **1970**, *92*, 2926.
(19) Norman, J. G.; Renzoni, G. E.; Case, D. A. *J. Am. Chem. Soc.* **1979**, *101*, 5259.

Table VII. Formation Constants of Me_2SO–$[Rh_2(ac)_n(acam)_{4-n}]^{0/+}$ Adducts in AN (0.1 M TBAP) at Room Temperature

compd	log K_1		log K_2		log K_1^+		log K_2^+	
	OP[a]	EC[a]	OP	EC	OP	EC	OP	EC
$Rh_2(ac)_4$	1.04	1.18	−0.22	−0.53	3.20	3.59	*b*	2.01
$Rh_2(ac)_3(acam)$	1.34	1.62	0.90	0.92	2.36	2.47	1.00	1.19
$Rh_2(ac)_2(acam)_2$	1.90	2.26	1.20	0.90	1.86	1.50	0.60	0.42
$Rh_2(ac)(acam)_3$	2.28	2.63	1.18	1.14	1.70	1.38	0.48	0.10
$Rh_2(acam)_4$	2.90	2.94	1.90	1.82	1.10	1.25	0.70	0.66

[a] Abbreviations: OP, optically determined; EC, electrochemically determined. [b] Cannot be determined due to decomposition of the oxidized complex on the spectrophotometric time scale in Me_2SO.

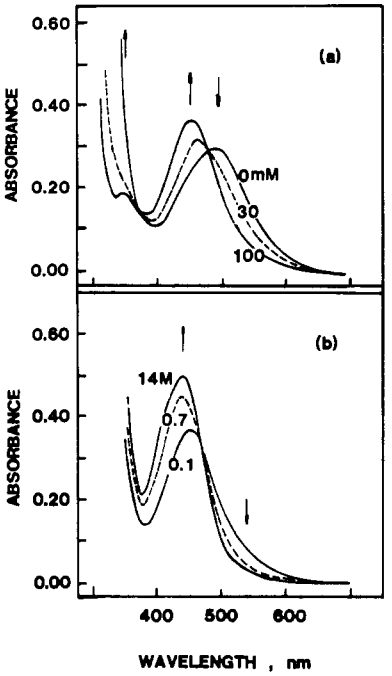

Figure 3. Spectral changes of $Rh_2(acam)_4$ in acetonitrile (0.1 M TBAP) during Me_2SO addition: (a) first ligand exchange (eq 1); (b) second ligand exchange (eq 2). Concentrations of Me_2SO are indicated on each spectrum.

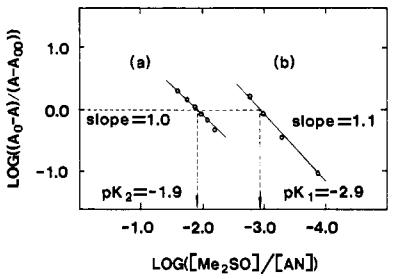

Figure 4. Logarithmic analysis of the spectral changes during Me_2SO additions to $Rh_2(acam)_4$ in acetonitrile. The actual spectra for this plot are given in Figure 3.

A log (absorbance) analysis of the data gives the number of added Me_2SO molecules for each step. These data are shown in Figure 4 and give a slope corresponding to one Me_2SO added. All other $Rh_2(ac)_n(acam)_{4-n}$ complexes were titrated in the same fashion, and the observed spectral changes were similar to those described above. Determined log K values for the series of complexes are listed in Table VII.

The singly oxidized $[Rh_2(ac)_n(acam)_{4-n}]^+$ species were electrochemically generated in AN, containing 0.1 M TBAP. This was done under a positive pressure of nitrogen. All of the singly oxidized complexes (n = 0–4) were found to be stable in AN. All of the $[Rh_2(ac)_n(acam)_{4-n}]^+$ species were found to be stable in pure Me_2SO except $[Rh_2(ac)_4]^+$. $[Rh_2(ac)_4]^+$ generated in pure Me_2SO, 0.1 M TBAP, was found to be unstable, and original spectra of $Rh_2(ac)_4^0$ could not be regenerated upon application of negative potentials.

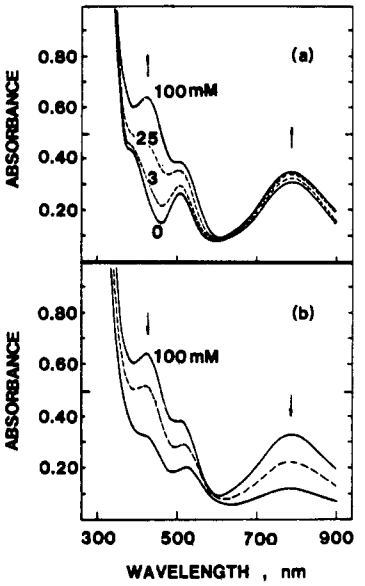

Figure 5. Spectral changes of $[Rh_2(ac)_4]^+$ in acetonitrile (0.1 M TBAP) during Me_2SO additions: (a) first ligand exchange (eq 4, Me_2SO concentration indicated on each spectrum); (b) decrease of absorbance indicating decomposition after Me_2SO concentration exceeds 0.1 M.

Spectral changes observed during the titration of $[Rh_2(ac)_4]^+$ with Me_2SO in AN are shown in Figure 5a. The solution spectrum of $[Rh_2(ac)_4]^+$ in pure acetonitrile, 0.1 M TBAP, has peaks at 797, 505, and ~390 nm. In Figure 5a it can be observed that the peak at about 797 nm does not shift up to an Me_2SO concentration of 0.1 M but only increases slightly in intensity. A new peak appears at 443 nm during the titration, and the original peak at 505 nm broadens to a shoulder and appears to lose intensity.

The fact that the peaks at 797 and 505 nm remain in the spectrum up to an Me_2SO concentration of 0.1 M may be taken as an indication of uncomplexed $[Rh_2(ac)_4]^+$ in solution. When this solution is allowed to stand in air at room temperature, the absorbing species slowly decomposes with a half-life of about 24 min. For Me_2SO concentrations ≥0.1 M the peaks at 443, 505, and 797 mm all lose intensity without showing any isosbestic behavior (Figure 5b). Thus, decomposition of $[Rh_2(ac)_4]^+$ appears to become dominant at these concentrations. If the concentration at which the peak at 443 nm reaches maximum intensity is taken to signal the saturation of equilibrium, an approximate value of $K_1^+ = 1.6 \times 10^3$ can be estimated. However, an inaccuracy arises due to the loss of the $[Rh_2(ac)_4]^+$ species and the true K_1^+ value could be higher than 1.6×10^3. A value of K_2^+ could not be determined due to decomposition.

Each of the $[Rh_2(ac)_n(acam)_{4-n}]^+$ complexes (n = 0–3) displays a high-intensity band in the 500-nm region in AN. This band loses intensity upon addition of Me_2SO, but no new bands appear in the visible region. However, new peaks do arise in the UV region and these can be used to monitor the titration. During the entire titration of $[Rh_2(acam)_4(AN)_2]^+$ by Me_2SO solutions, a new absorbance peak continuously grows in intensity at a wavelength of ~280 nm. Yet, in AN, two different isosbestic points appear at different ranges of Me_2SO concentrations. No single absorbance peak can be assigned to a mono(dimethyl sulfoxide)

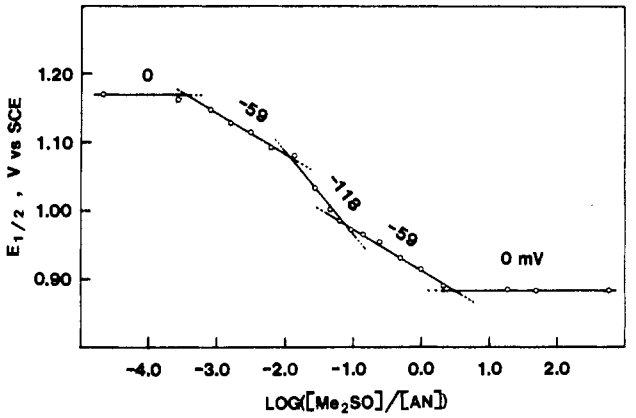

Figure 6. Dependence of the first oxidation potential of $Rh_2(ac)_4$ on the Me_2SO/AN ratio in solutions containing 0.1 M TBAP.

adduct. This is similar to the titrations of neutral $Rh_2(ac)_n(acam)_{4-n}$ complexes. The same feature is also observed in the titration of $[Rh_2(ac)(acam)_3]^+$, $[Rh_2(ac)_2(acam)_2]^+$, and $[Rh_2(ac)_3(acam)]^+$. The determined log K^+ values are listed in Table VII.

From Table VII, it can be clearly seen that the log K_1 (eq 1) values increase with an increase in the number of acetamidate ligands. There is, however, an opposite trend for the log K_1^+ values (eq 4). The log K_2 values and the log K_1^+ values may not be very accurate, due to the fact that those values are very small, as well as due to the uncertainty of the initial absorbance (A_0) spectrum for the formation of a bis(dimethyl sulfoxide) adduct. This spectrum is used in the calculations, and any error in the nature of this spectrum would enhance the inaccuracy of the determinations.

Electrochemical Studies of $Rh_2(ac)_n(acam)_{4-n}$ in Mixed Me_2SO/AN Solutions. Electrochemistry is an excellent method for determining stability constants of complexed inorganic ions. For the singly oxidized complexes investigated in this study, there was some experimental difficulty in spectrally determining the values of K_2. Thus, these values were determined electrochemically. At the same time, values of K_1 and K_2 for the neutral $Rh_2(ac)_n(acam)_{4-n}$ complexes as well as K_1 for the singly oxidized complexes were determined. These data provided a good verification of the spectrally obtained values and also give direct information as to whether the HOMO is raised or lowered as a result of Me_2SO binding.

Half-wave potentials for the first oxidation step of each $Rh_2(ac)_n(acam)_{4-n}$ complex in Me_2SO and in AN have been reported.[7] Cyclic voltammograms of $Rh_2(ac)_n(acam)_{4-n}$ complexes with n = 0–4 in both AN and Me_2SO solutions containing 0.1 M TBAP gave about a 60-mV peak separation between the anodic and cathodic peaks (ΔE_p) for the first oxidation when the scan rate is 100 mV/s. This separation implies that the electron-transfer reactions in both solvents are reversible.

Formation constants of Me_2SO adducts can be electrochemically determined by monitoring shifts in half-wave potential as a function of the concentration of free Me_2SO.[20,21] A plot of $E_{1/2}$ vs. log ([Me_2SO]/[AN]), in theory, should have slopes of $\pm 0.059f$ V/log unit, where f is the number of Me_2SO and AN molecules exchanged in the course of oxidation. Such plots are shown in Figures 6 and 7. The original data points were used to draw lines with Nernstian slopes. Such plots were then used to arrive at the values of K_1, K_2, β_2 and K_1^+, K_2^+, β_2^+. These values are listed in Table VII and compare well with those obtained spectroscopically, thus justifying the discussion below.

Potentials were measured by cyclic voltammetry during the Me_2SO titration of the dirhodium complexes in AN solutions. As shown in Figure 6, the half-wave potential for oxidation of

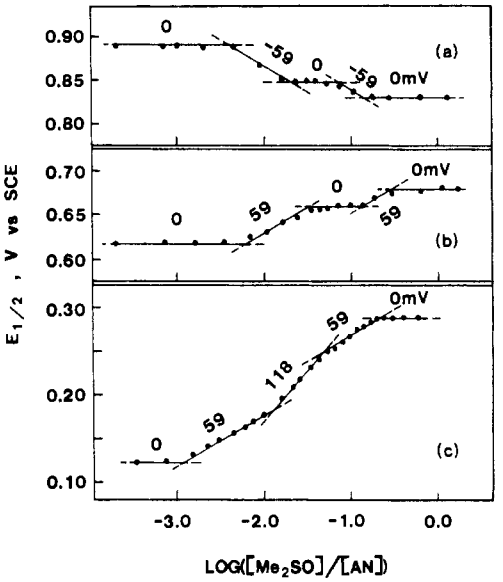

Figure 7. Variation of the oxidation potential of $Rh_2(ac)_n(acam)_{4-n}$ in Me_2SO–AN mixtures containing 0.1 M TBAP: (a) $Rh_2(ac)_3(acam)$; (b) $Rh_2(ac)_2(acam)_2$; (c) $Rh_2(acam)_4$.

$Rh_2(ac)_4$ in Me_2SO–AN is shifted negatively with increase in the Me_2SO/AN ratio. Five steps are shown with slopes of 0, −59, −118, −59, and 0. These slopes correspond to the case where the Me_2SO ligands bound to the oxidized species are in excess of those bound to the neutral complex (over the corresponding concentration ranges). This conclusion is derived from the negative slopes which are in integral multiples of 59 mV/log [(Me_2SO)/(AN)].[20,21]

In the absence of Me_2SO, the dirhodium complex shows a reversible redox reaction and no ligand exchange occurs during the oxidation. Under these conditions the electrode reaction is given as

$$Rh_2(ac)_4(AN)_2 \rightleftarrows [Rh_2(ac)_4(AN)_2]^+ + e^- \quad (7)$$

As indicated by the negative slopes in Figure 6, Me_2SO binds to the oxidized form of the complex [$Rh^{II\,1/2}$–$Rh^{II\,1/2}$] more strongly than to the reduced form of the complex [Rh^{II}–Rh^{II}] and thus the one ligand-exchange (slope −59 mV/log unit) process that takes place at increased Me_2SO concentration is

$$Rh_2(ac)_4(AN)_2 + Me_2SO \rightleftarrows [Rh_2(ac)_4(AN)(Me_2SO)]^+ + e^- + AN \quad (8)$$

An exchange of two ligands (slope −118 mV/log unit) can accompany the oxidation at higher Me_2SO concentrations:

$$Rh_2(ac)_4(AN)_2 + 2Me_2SO \rightleftarrows [Rh_2(ac)_4(Me_2SO)_2]^+ + e^- + 2AN \quad (9)$$

Finally, when the concentration of Me_2SO reaches a value where the neutral dirhodium complex is mainly in the form of a mono(dimethyl sulfoxide) adduct, the two-ligand-exchange process disappears and a one-ligand exchange again occurs. The overall mechanism is

$$Rh_2(ac)_4(AN)(Me_2SO) + Me_2SO \rightleftarrows [Rh_2(ac)_4(Me_2SO)_2]^+ + e^- + AN \quad (10)$$

At very high concentrations of Me_2SO, the dirhodium species are complexed by two Me_2SO molecules and no ligand-exchange process occurs during the oxidation. The electrode reaction is then represented by eq 11.

$$Rh_2(ac)_4(Me_2SO)_2 \rightleftarrows [Rh_2(ac)_4(Me_2SO)]^+ + e^- \quad (11)$$

Combining eq 7–11 gives a mechanism over the entire range of Me_2SO concentrations. This mechanism is represented in Scheme I, where A = AN, D = Me_2SO, and the numbers 7–11 correspond to the equations in the text. Formation constants for both the oxidized and reduced forms of the dirhodium complex

(20) Galus, Z. *Fundamentals of Electrochemical Analysis*; Ellis Harwood: New York, 1976; pp 360–379.
(21) Crow, D. R. *Polarography of Metal Complexes*; Academic: London, 1969.

Scheme I. Electron-Transfer and Ligand-Exchange Mechanism of $Rh_2(ac)_4$ in AN–Me_2SO Solvent Systems

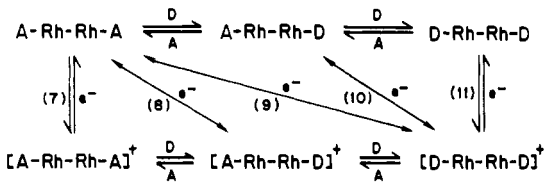

Scheme II. Electron-Transfer and Ligand-Exchange Mechanism of $Rh_2(ac)_3(acam)$ in AN–Me_2SO Solvent Systems

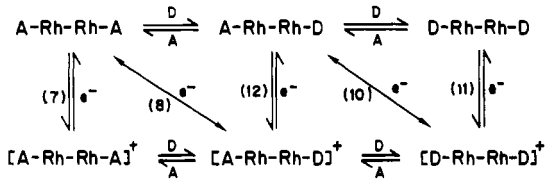

Scheme III. Electron-Transfer and Ligand-Exchange Mechanism of $Rh_2(ac)_2(acam)_2$ and $Rh_2(ac)(acam)_3$ in AN–Me_2SO Solvent Systems

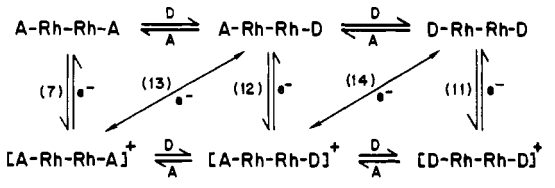

were calculated with use of the mechanism in Scheme I and the data presented in Figure 6.[20,21] These calculations give values of $\log K_1 = 1.18$, $\log K_2 = -0.53$, $\log K_1^+ = 3.59$, and $\log K_2^+ = 2.01$. Reasonably good agreement can be seen between these values calculated from the electrochemical results and those determined by optical methods (Table VII). The formation constants in Table VII are consistent with the proposed mechanism in Scheme I and demonstrate the greatly enhanced binding ability of Me_2SO by the singly oxidized $[Rh_2(ac)_4]^+$.

A systematic study of the oxidation mechanism for the complete series of dirhodium complexes was carried out in the same way. Figure 7a shows the concentration dependence of $E_{1/2}$ for the $Rh_2(ac)_3(acam)$ oxidation in a mixed Me_2SO–AN solvent system. There is a shift of $E_{1/2}$ in five regions having different slopes. However, a zero-slope region appears in the intermediate-concentration region rather than the −118-mV slope found in Figure 6. The reaction in this region is represented by eq 12. A corresponding mechanism is proposed as shown in Scheme II, where A = AN and D = Me_2SO.

$$Rh_2(AN)(Me_2SO) \rightleftarrows [Rh_2(AN)(Me_2SO)]^+ + e^- \quad (12)$$

The titrations of acetonitrile solutions of $Rh_2(ac)_n(acam)_{4-n}$ complexes having $n \leq 2$ with Me_2SO give results that are significantly different from those discussed above. For complexes with $n > 2$ the slopes of $E_{1/2}$ vs. log ([Me_2SO]/[AN]) are negative (Figures 6 and 7a) while for those with $n \leq 2$ the slopes are positive (Figure 7b,c), indicating that, in the latter complexes, Me_2SO binds more strongly to the dirhodium(II) form than the dirhodium($II^1/_2$).

Figure 7b shows the shift of $E_{1/2}$ during the titration of an AN solution of $Rh_2(ac)_2(acam)_2$ with Me_2SO. Five regions with positive slopes of 0, 59, 0, 59, and 0 mV are observed. Equations 13 and 14 are written to describe the two reactions giving slopes

$$Rh_2(AN)(Me_2SO) + AN \rightleftarrows [Rh_2(AN)_2]^+ + Me_2SO + e^- \quad (13)$$

$$Rh_2(Me_2SO)_2 + AN \rightleftarrows [Rh_2(AN)(Me_2SO)]^+ + Me_2SO + e^- \quad (14)$$

of +59 mV. Almost the same features have been found for the $Rh_2(ac)(acam)_3$ system, and the corresponding mechanism is shown in Scheme III, where A = AN and D = Me_2SO.

Scheme IV. Electron-Transfer and Ligand-Exchange Mechanism of $Rh_2(acam)_4$ in AN–Me_2SO Solvent Systems

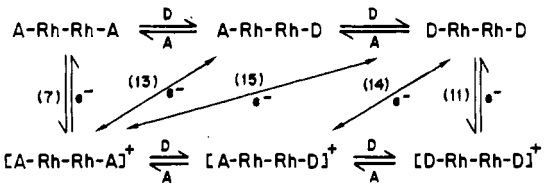

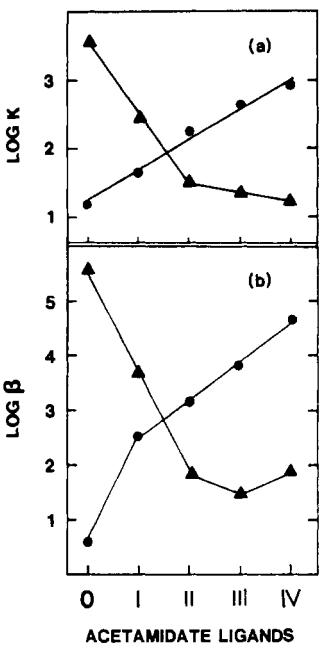

Figure 8. Variation of formation constants on the number of bridging (acetamidate) ligands in the $[Rh_2(ac)_n(acam)_{4-n}]^{0/+}$ complexes: (a) K_1 (●) and K_1^+ (▲); (b) β_2 (●) and β_2^+ (▲). The actual values are given in Table VII.

Figure 7c shows the positive shift of $E_{1/2}$ with increasing Me_2SO concentrations for $Rh_2(acam)_4$ oxidation in the Me_2SO–AN system. The zero or positive slope of $E_{1/2}$ with increasing [Me_2SO] over the entire Me_2SO concentrations range suggests a mechanism exactly opposite to the case of $Rh_2(ac)_4$ (Figure 6, Scheme I). Here eq 15 can be written to describe the reaction giving rise to

$$Rh_2(Me_2SO)_2 + 2AN \rightleftarrows [Rh_2(AN)_2]^+ + 2Me_2SO + e^- \quad (15)$$

a slope of +118 mV. This proposed mechanism is shown in Scheme IV. All of the electrochemically determined formation constants are summarized in Table VII.

Figure 8a shows the relationship between $\log K_1$, $\log K_1^+$, and the number of acetamidates in the bridging ligands. Figure 8b shows the relationship between $\log \beta_2$, $\log \beta_2^+$, and the number of acetamidates in the bridging ligands. The electrochemically determined data are used in this figure, but similar trends are obtained from the spectroscopic data.

Significance of the Trends in Binding Constants. It can be seen that the $\log K_1$ values increase monotonically on going from $Rh_2(ac)_4$ to $Rh_2(acam)_4$. The $\log \beta_2$ values show a similar increase on going from $Rh_2(ac)_4$ to $Rh_2(acam)_4$. The $\log K_1^+$ values show an opposite trend. It can be generally noted that, for $Rh_2(ac)_4$, $\log K_1 << \log K_1^+$ and $\log \beta_2 << \log \beta_2^+$. For $Rh_2(acam)_4$, $\log K_1 >> \log K_1^+$ and $\log \beta_2 >> \log \beta_2^+$. Other complexes between $Rh_2(ac)_4$ and $Rh_2(acam)_4$ show an intermediate behavior.

The opposite trends in the magnitudes of $\log K_1$ and $\log K_1^+$ or $\log \beta_2$ and $\log \beta_2^+$ (Figure 8) are significant. In the neutral $Rh_2(ac)_4(Me_2SO)_2$ complex ($n = 4$), the crystal structure shows that Me_2SO binding occurs via the sulfur atom. The same mode of binding occurs for $Rh_2(acam)_4(Me_2SO)_2$. This is shown by the crystal structure reported in this paper. The Rh–S distance in $Rh_2(acam)_4(Me_2SO)_2$ is 2.414 Å while the Rh–S distance in

$Rh_2(ac)_4(Me_2SO)_2$ is 2.451 Å. This difference in binding strength of the Rh_2–Me_2SO bonds is reflected in the binding constants. Clearly, the Rh atoms in $Rh_2(acam)_4$ are "softer" than in $Rh_2(ac)_4$ and this is reflected in oxidation potentials of these complexes.[7]

The one-electron oxidation of the above two complexes is expected to result in the following: (a) the rhodium centers in the oxidized, dirhodium($II^1/_2$), species of each should be harder than the respective neutral dirhodium(II) species, and (b) the rhodium centers in $[Rh_2(ac)_4]^+$ should be harder than in $[Rh_2(acam)_4]^+$. Considering that the "harder" $Rh_2(ac)_4$ has a smaller log K_1 or log β_2 for Me_2SO binding than $Rh_2(acam)_4$ and (b) above, the magnitudes of the respective log K_1^+ and log β_2^+ should show a change in the same direction *provided that, after oxidation, Me_2SO remains bound via S atoms.* Values of formation constants in Table VII show that the decrease in binding constants on going from $Rh_2(acam)_4$ to $[Rh_2(acam)_4]^+$ is consistent with (a) above and Me_2SO binding via S atom(s). Thus, both Me_2SO molecules in $[Rh_2(acam)_4(Me_2SO)_2]^+$ may be bound to the rhodium centers via S atoms. In contrast, on going from $Rh_2(ac)_4$ to $[Rh_2(ac)_4]^+$ the binding constants increase, suggesting that at least one Me_2SO molecule in $[Rh_2(ac)_4(Me_2SO)_2]^+$ is not bound via an S atom.

In an earlier report,[7] we noted that the $E_{1/2}$ value of $Rh_2(ac)_4$ in Me_2SO was consistent with its Gutmann donor number[8] but that the oxidation potential for $Rh_2(acam)_4$ is ~230 mV more positive than that expected from the donor number trend. Since the donor number for Me_2SO is valid only when it is bound via the oxygen atom, this mode of Me_2SO binding appears to be important in the $E_{1/2}$ value for oxidation of $Rh_2(ac)_4$. The suggestion that Me_2SO is bound via the oxygen atom to $[Rh_2(ac)_4]^+$ and the preceding observation are mutually supportive.

It may be noted that the $[Rh_2(ac)_4]^{+/0}$ redox couple in pure Me_2SO shows characteristics of a reversible process.[7] Yet, the neutral form is believed to be S bound to Me_2SO in solution while the singly oxidized form seems to bind via the O atom. The change of the Me_2SO linkage appears not to hinder the rate of electron transfer and hence may be kinetically facile.

The other three complexes with $n = 1$–3 show a behavior that is between those for complexes having $n = 0$ and 4 discussed above. The binding constants for $Rh_2(ac)_3(acam)$ increase upon oxidation in a manner similar to that for $Rh_2(ac)_4$ but to a smaller extent. $Rh_2(ac)_2(acam)_2$, on the other hand, shows a decrease in binding constant upon oxidation similar to that for $Rh_2(acam)_4$, but also to a smaller extent. These intermediate cases may imply that both modes of Me_2SO binding may be present in the oxidized state. In fact, combinations of S–Rh–Rh–S, S–Rh–Rh–O, and O–Rh–Rh–O species may be present in fluxional equilibria with all of the oxidized complexes of the $Rh_2(ac)_n(acam)_{4-n}$ series. This is consistent with ESR spectra of $[Rh_2(ac)_n(acam)_{4-n}]^+$ (n = 3–0) in Me_2SO, which appear to show more than one set of axial spectra.[7] The tendency toward such fluxionality in the neutral $Rh_2(ac)_4$ complex solution may explain why the linkage change during the $[Rh_2(ac)_4]^{0/+}$ cycle does not limit the rate of electron transfer.

Comments about π Interaction. The structural data, electrochemical measurements, and binding constants reported in this paper can all be rationalized on the basis of "softness" or "hardness" of each acid and base involved in adduct formation. Measurement of reversible potentials for the oxidation of $Rh_2(acam)_4$ in the absence of axial ligands should provide a means for detecting a lowering or raising of the HOMO when axial ligands are present. This important piece of information is unavailable because $Rh_2(acam)_4$ is insoluble in nonbonding solvents. Hence, the discussion of potential shifts as one goes from CH_3CN to Me_2SO is limited to differences in binding constants of the neutral vs. the singly oxidized complexes. In this paper, no assertions can be made regarding π interaction between rhodium centers and the σ-bound Me_2SO molecules. However, a study of CO adducts of similar dirhodium complexes[22] indeed suggests that the HOMO is lowered upon CO binding. In light of this, most of the data presented here may also be rationalized in terms of π interactions or a lack thereof.

Acknowledgment. This work was supported by the Robert A. Welch Foundation (K.M.K., Grant No. E-680; J.L.B., Grant No. E-918; I.B., Grant No. E-594).

Registry No. Me_2SO, 67-68-5; $Rh_2(ac)_4$, 15956-28-2; $Rh_2(ac)_3(acam)$, 87985-37-2; $Rh_2(ac)_2(acam)_2$, 87985-38-4; $Rh_2(ac)(acam)_3$, 87985-39-5; $Rh_2(acam)_4$, 87985-40-8; $Rh_2(ac)_4^+$, 83681-59-8; $Rh_2(ac)_3(acam)^+$, 87985-41-9; $Rh_2(ac)_2(acam)_2^+$, 87985-42-0; $Rh_2(ac)(acam)_3^+$, 87985-43-1; $Rh_2(acam)_4$, 87985-44-2; $Rh_2(ac)_4(MeCN)_2$, 80419-75-6; $Rh_2(ac)_3(acam)(MeCN)_2$, 92525-89-8; $Rh_2(ac)_2(acam)_2(MeCN)_2$, 92525-90-1; $Rh_2(ac)(acam)_3(MeCN)_2$, 92525-91-2; $Rh_2(acam)_4(MeCN)_2$, 92525-88-7; $Rh_2(ac)_4(MeCN)_2^+$, 92526-07-3; $Rh_2(ac)_3(acam)(MeCN)_2^+$, 92526-00-6; $Rh_2(ac)_2(acam)_2(MeCN)_2^+$, 92526-01-7; $Rh_2(ac)(acam)_3(MeCN)_2^+$, 92526-02-8; $Rh_2(acam)_4(MeCN)_2^+$, 92526-03-9; $Rh_2(ac)_4(Me_2SO)_2$, 26023-60-9; $Rh_2(ac)_3(acam)(Me_2SO)_2$, 92525-94-5; $Rh_2(ac)_2(acam)_2(Me_2SO)_2$, 92525-95-6; $Rh_2(ac)(acam)_3(Me_2SO)_2$, 92525-96-7; $Rh_2(acam)_4(Me_2SO)_2$, 100992-47-0; $Rh_2(ac)_4(Me_2SO)_2^+$, 92526-08-4; $Rh_2(acam)_4(Me_2SO)_2^+$, 92526-06-2; MeCN, 75-05-8.

Supplementary Material Available: Listings of anisotropic thermal parameters, root-mean-square amplitudes of thermal vibration, and observed and calculated structure factors (29 pages). Ordering information is given on any current masthead page.

(22) Chavan, M. Y.; Ahsan, M. Q.; Lifsey, R. S.; Bear, J. L.; Kadish, K. M. *Inorg. Chem.*, in press.